

## Climatological diurnal variability in sea surface temperature characterized from drifting buoy data

S. Morak-Bozzo<sup>1\*</sup>, C. J. Merchant<sup>1,2</sup>, E. C. Kent<sup>3</sup>, D. I. Berry<sup>3</sup> and G. Carella<sup>3</sup>

<sup>1</sup>Department of Meteorology, University of Reading, Reading, UK

<sup>2</sup>National Centre for Earth Observation, University of Reading, Reading, UK

<sup>3</sup>National Oceanography Centre, Southampton, UK

\*Correspondence: S. Morak-Bozzo, Harry Pitt Building, 3 Earley Gate, PO Box 238, Whiteknights, Reading, RG6 6AL, UK  
E-mail: s.morak@reading.ac.uk

This article was funded by the National Environment Research Council (NERC), grant numbers NE/J02306X/2 and NE/J020788/1.

### Abstract

Drifting buoy sea-surface temperature (SST) records have been used to characterize the diurnal variability of ocean temperature at a depth of order 20 cm. We use measurements covering the period 1986–2012 from the International Comprehensive Ocean-Atmosphere Data Set (ICOADS) version 2.5, which is a collection of marine surface observations that includes individual SST records from drifting buoys. Appropriately transformed, this dataset is well suited for estimation of the diurnal cycle, since many drifting buoys have high temporal coverage (many reports per day), and are globally distributed. For each drifter for each day, we compute the local-time daily SST variation relative to the local-time daily mean SST. Climatological estimates of subdaily SST variability are found by averaging across various strata of the data: in 10° latitudinal bands as well as globally; and stratified with respect to season, wind speed and cloud cover. A parameterization of the diurnal variability is fitted as a function of the variables used to stratify the data, and the coefficients for this fit are also provided with the data. Results are consistent with expectations based on the previous work: the diurnal temperature cycle peaks in early afternoon (circa 2 pm local time); there is an increase in amplitude and a decrease in seasonality towards the equator. Generally, the ocean at this depth cools on windy days and warms on calm days, so that a component of subdaily variability is the SST tendency on slower timescales. By not ‘closing’ the diurnal cycle when stratified by environmental conditions, this dataset differs from previously published diurnal-cycle parameterizations. This thorough characterization of the SST diurnal cycle will assist in interpreting SST observations made at different local times of day for climatological purposes, and in testing and constraining models of the diurnal-cycle and air-sea interaction at high temporal resolution.

*Geosci. Data J.* **3**: 20–28 (2016), doi: 10.1002/gdj3.35

Received: 25 August 2015, revised: 20 April 2016, accepted: 3 May 2016

**Key words:** SST, diurnal variations, drifting buoys

### Dataset

Identifier: <http://dx.doi.org/10.6084/m9.figshare.2069049>

Creator: S Morak-Bozzo

Title: Diurnal SST anomalies

Publisher: Figshare

Publication year: 2015

Resource type: Dataset

Version: V1.1

## 1. Data production methods

Diurnal variations in sea-surface temperature (SST) influence air-sea interaction and mean climate.

Unaccounted for, diurnal variations may cause artefacts in climate data records of SST, which is the immediate motivation of the work presented in this paper. Our aim is to characterize diurnal SST variability

at depths characteristic of many *in situ* SST observations (drifting buoys, and traditional bucket observations from ships).

To this end, drifting buoy data, from the ICOADS release 2.5 (Woodruff *et al.*, 2011) are used. The individual record of each buoy includes the buoy identification number, the date and time in universal time coordinates (UTC), the location, given in degree latitude and longitude, rounded to the second decimal place and the measured SST rounded to the first decimal place. The records cover the period 1986–2012.

In addition to the sea-surface temperature SST records, 6-h fields of 10 m wind speed and total cloud cover from the ECMWF reanalysis (ERA) Interim are used (Dee *et al.*, 2011). ERA Interim has a spatial resolution of 1.5°.

### 1.1. Analysis

The analysis of the daily diurnal cycle for each drifting buoy is performed individually following the procedure described below.

The time is converted from UTC to mean local solar time, then the observations are binned into hourly bins. Hourly anomalies are computed by subtracting the local-time daily mean SST from each SST value. The computation of anomalies relative to a daily mean for each individual buoy is assumed to remove effects of drifting buoy calibration errors, which are typically of order 0.15–0.19 K (Lean and Saunders, 2013) and often change progressively during a drifting buoy's lifetime. In order to ensure a valid daily mean for computing anomalies, only records with at least one observation within each quarter of the day (0000–0006, 0006–0012 h, etc) are retained.

The retained records are then aggregated in various bins. Annual and seasonal (DJF, MAM, JJA, SON) values of the diurnal SST cycle are determined by computing the median over all retained records in each hourly bin through the day. The data are also variously subdivided by latitude, cloud cover and wind speed, as explained further below. The median is used since it is less biased by occasional outliers, which makes minimal difference in most cases, but is more robust for some sparsely populated bins. Some outliers arise because of extreme (>5 K) diurnal-cycle events (Merchant *et al.*, 2008). Extreme individual events are not the focus of this climatological study. Our concern is to characterize diurnal cycles climatologically, for use with relatively limited contextual information.

If a median bin value is used as an estimate of the diurnal cycle, there is a statistical uncertainty in this estimate arising from variability of the diurnal cycle with factors not accounted for by the binning. This uncertainty is estimated by the median absolute deviation from the median (*MADM*) scaled to give a robust standard deviation estimate (e.g. Rousseeuw and Croux, 1993):

$$\sigma_{\text{robust}} = \text{MADM} \times 1.4826.$$

Another quantity of interest is standard uncertainty in the bin median,  $U_{\text{bin}}$  (measuring how well the average diurnal cycle is estimated for a given hour). This is dependent on the variability and on the sample size,  $n$ , and is estimated, by analogy to 'standard error in the mean', by:

$$U_{\text{bin}} = \sigma_{\text{robust}} / \sqrt{n}.$$

Here,  $n$  is the number of distinct bin records contributing to the bin median.

The diurnal SST cycle is computed both globally and in 10° latitudinal bands. We also explore the influence of varying wind speed and cloud cover conditions on the diurnal SST variations by further subdividing the data. We choose four wind speed (Table 1) and 12 combined wind speed and cloud cover categories (Table 2).

For the analysis stratified by wind speed or both wind speed and cloud cover conditions, match-ups of the ERA Interim fields (Dee *et al.*, 2011) with the buoy SST observation are determined. To begin with the ERA Interim grid cell nearest to each buoy observation and the two 6-hourly records, closest to noon local time, are selected from the reanalysis output. Then, a linear interpolation is performed to estimate the wind speed/total cloud cover at local midday. The noon values of wind speed/total cloud cover are paired with the drifter SST data. The computation of the diurnal SST cycle is repeated, stratifying the data based on wind speed only or wind speed and total cloud

**Table 1.** Wind speed ( $u$ ) categories.

Categories	$u$ (m/s)
1	0–3
2	3–7
3	7–12
4	>12

**Table 2.** Combined total cloud cover ( $C$ ) and wind speed ( $u$ ) categories.

Categories	$C$ (%)	$u$ (m/s)
1	0–20*	0–3
2	0–20	3–7
3	0–20	7–12
4	0–20	>12
5	20–80†	0–3
6	20–80	3–7
7	20–80	7–12
8	20–80	>12
9	80–100‡	0–3
10	80–100	3–7
11	80–100	7–12
12	80–100	>12

\*Clear.

†Cloudy.

‡Overcast.

cover together. Use of noon conditions for the stratification by environmental conditions is motivated by: simplicity; the period around this time (0010–0014 h) being highly influential on the amplitude of diurnal cycle obtained (Gentemann *et al.*, 2003); and the common availability of local noon weather reports for historic ship observations of SST (Wilkinson *et al.*, 2011).

## 1.2. Results

The results without stratification by wind speed or cloud cover show an increase in the amplitude of diurnal variations of SSTs towards the equator and a decrease in the differences between seasons (Figure 1). Figure 1 also shows that the diurnal variation 'closes' in the annual average at midlatitudes, whereas, for example, on a typical day between March

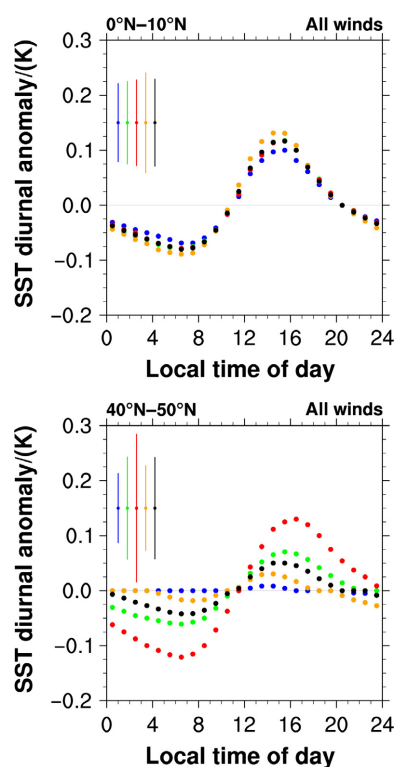


**Figure 1.** All-conditions average of diurnal cycle of daily SST anomalies for the latitudinal bands 0°N–10°N and 40°N–50°N. The annual mean diurnal cycle is displayed in black, Northern Hemisphere winter (DJF) in blue, spring (MAM) in green, summer (JJA) in red and autumn (SON) in orange. The bars in the top left corner, show the associated uncertainties. The length of the thin uncertainty bars shows the daily mean of the hourly robust standard deviations (thin line), indicating the typical uncertainty in applying the bin median as an estimate of the diurnal cycle. The standard uncertainty in the bin median is given by the extent of the thick uncertainty bar (although in these plots, the standard uncertainties are so small that the uncertainty bar appears as a dot). The bars are colour-coded for each season and the annual mean, following the colour code of the diurnal cycle data.

and May, the sea at 20 cm is 0.1 K warmer at the end of the day than at the start. The asymmetry of the diurnal cycle curves of the intermediate seasons (spring, MAM, and autumn, SON), reflects the warming tendency of the ocean during spring (green markers in Figure 1) and the onset of cooling after the August SST maximum (orange markers in Figure 1).

Note also in the lower panel of Figure 1 that the larger magnitude of the diurnal cycle in summer also corresponds to higher variability in the diurnal cycle around the average case (thin uncertainty bars). This reflects greater diurnal stratification and variability in that stratification wind speed, including occasional extreme warming events, when daytime solar heating of the surface is more intense. The uncertainty in the bin median is generally smaller than the dot sizes on the plot (which is also reflected in the smooth variation in the data through the day).

The results of the wind-stratified analysis, as shown in Figure 2 for the global diurnal SST cycle, feature a decrease in magnitude of the diurnal SST variations with increasing wind speed. The global mean diurnal cycle shows little seasonal change.

Figure 2 also shows that the variability around the median diurnal SST cycle is roughly proportional to the cycle's magnitude. Again, the uncertainty in the bin median is small.

We note in passing that Figure 2 further highlights the close agreement between the daily mean in the diurnal SST cycle, which is defined to be equal to zero, and the arithmetic mean of the anomalies at 10.30 am and 10.30 pm (see value in top right corner). This justifies the strategy for standardizing satellite overpass times to 10.30 am/10.30 pm used by Merchant *et al.* (2012), when developing decadal time series of SST for climate applications by remote sensing.

The outcome of the combined wind speed and cloud cover analysis of the diurnal SST variability, demonstrated by the example of latitudinal bands 40°S–30°S (Figure 3) and 30°N–40°N (Figure 4), shows a decrease in magnitude of diurnal cycle with increase in wind speed (Figure 3 and 4, left to right) as well as with cloud cover (Fig. 3, top to bottom). Wind speed conditions exert a larger influence over their range of variability on the diurnal cycle amplitude than do cloud cover conditions. A warming/cooling trend can be seen on calm/windy days. A comparison of the two displayed bands (Figure 3 and 4) shows a larger diurnal cycle amplitude for given wind and cloud conditions in the Northern Hemisphere than in the Southern Hemisphere for equivalent latitudinal bands. We speculate that may arise because there is more surface mixing from long-range wave propagation in the Southern Hemisphere, where there is less land and distances to coasts are greater. This is an aspect of diurnal variability that is not captured if a diurnal cycle model is driven only by solar insolation (represented here via cloud cover) and wind speed.

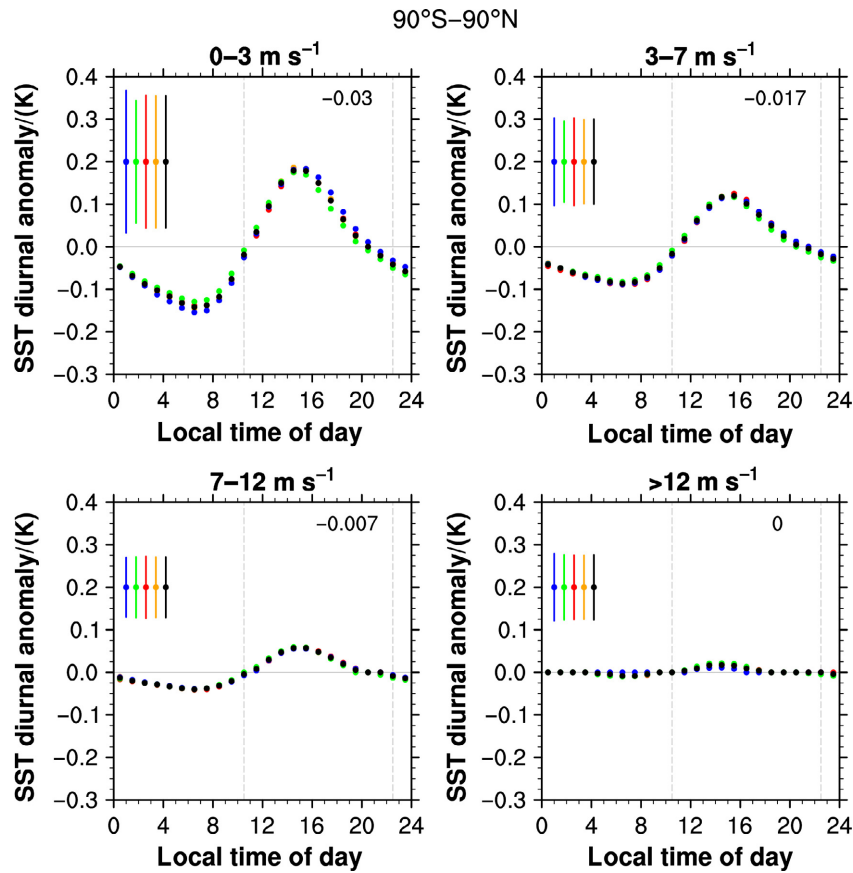


**Figure 2.** Global mean diurnal cycle of daily SST anomalies for wind speeds, (top left) 0–3 m/s, (top right) 3–7 m/s, (bottom left) 7–12 m/s and (bottom right) >12 m/s. The symbols are the same as for Figure 1. Vertical dashed lines mark the 1030 and 2230 h and the number in top left corner gives the arithmetic mean of the diurnal cycle at these two times.

The estimates of robust standard deviation (variability of the diurnal cycle) and robust standard uncertainty (uncertainty in the average cycle) are included in the dataset.

### 1.3. Fitting the diurnal SST cycle data

The dataset includes tabulations of the diurnal cycle of the SST. We have also parameterized the data. This allows computation of the SST diurnal anomaly as a smoothly varying function of time of day, wind speed and total cloud cover. The fitting is done by ordinary least squares minimization.

Previous works by Lindfors *et al.* (2011) and Kennedy *et al.* (2007) use a second-order Fourier series, to fit the diurnal SST cycle as a function of time. This approach, however, does not take into account the influence of varying wind speed and cloud cover conditions on the diurnal SST anomalies.

We fit the average diurnal SST anomalies using a polynomial function, a function of time, wind speed and cloud cover, with an additional linear trend. The trend was added to account for the observed warming/cooling tendency across the day during mid- and high-latitude seasons.

The fitted equation is:

$$\begin{aligned}
 SST_{anomaly2} = & \alpha_0 + \alpha_1 u + \alpha_2 C + \alpha_3 t + \alpha_4 ut + \alpha_5 Ct \\
 & + (\alpha_6 \times \sin(wt) + \alpha_7 C \sin(wt) + \alpha_8 \\
 & \times \cos(wt) + \alpha_9 C \cos(wt) + \alpha_{10} \sin(2wt) \\
 & + \alpha_{11} C \sin(2wt) + \alpha_{12} \cos(2wt) \\
 & + \alpha_{13} C \cos(2wt)) \times \exp\left(-\frac{u}{u_{avg}}\right),
 \end{aligned}
 \tag{1}$$

where  $\alpha_0 \dots \alpha_{13}$  are the fitting coefficients.  $u$  and  $C$  are the noon wind speed and total cloud cover values.  $u_{avg}$  is the average wind speed over all categories for a given latitudinal band and season.

The fitting process results in one set of fitting coefficients ( $\alpha_0 \dots \alpha_{13}$ ) for each latitudinal band and season. The form of Equation (1) draws on Gentemann *et al.* (2003) and Filipiak *et al.* (2012).

For a review of alternative parameterizations, refer to Kawai and Wada (2007), which also surveys the physics and modelling diurnal stratification. Alternative empirical formulations include those of Clayson and Curry (1996) and Li *et al.* (2001), both of which build on work by Webster *et al.* (1996). Stuart-Menteth *et al.* (2003), meanwhile, built on the formula for diurnal warming proposed by Kawai and Kawamura (2003).

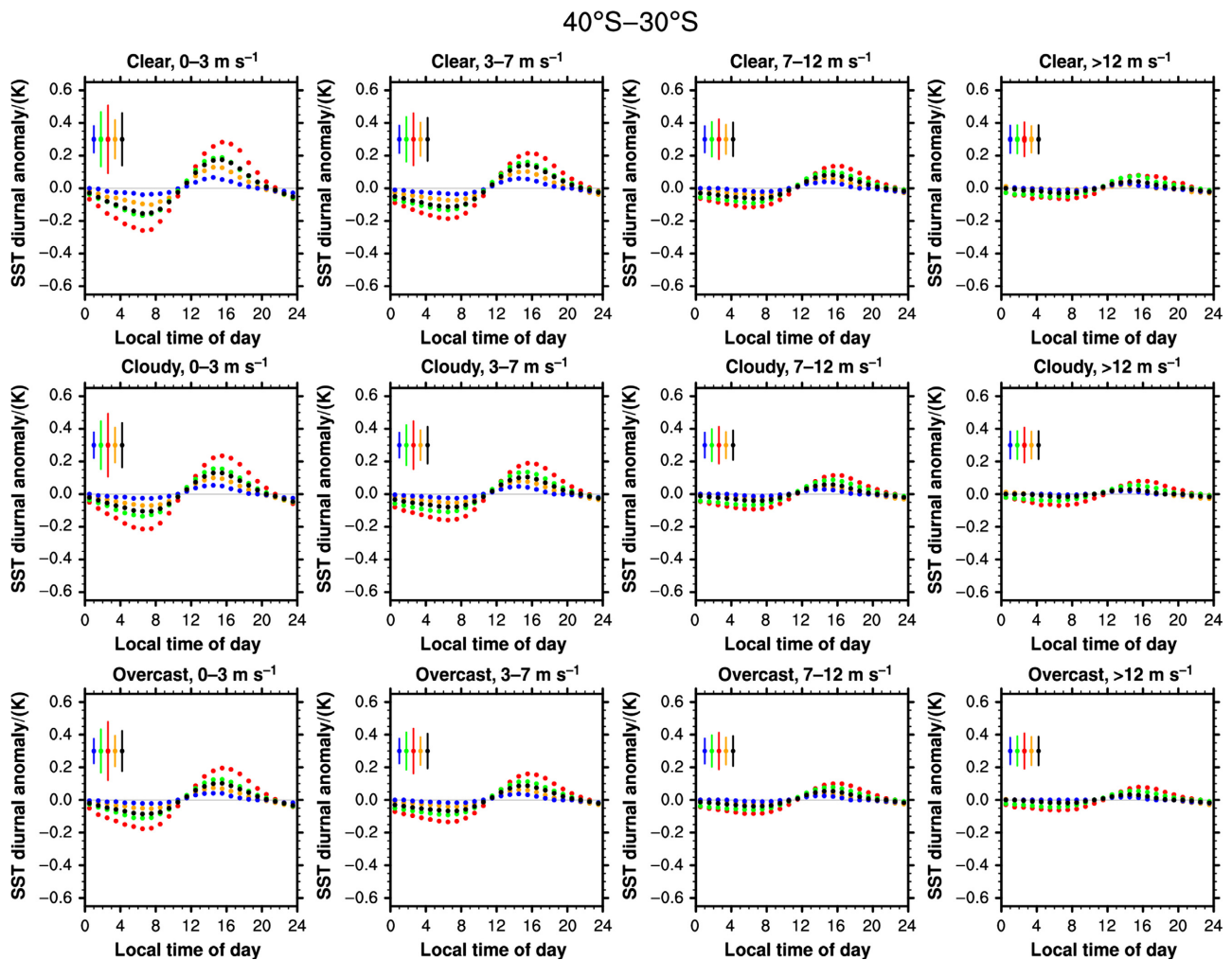


**Figure 3.** Diurnal cycle of daily SST anomalies between 40°S and 30°S for the 12 combined wind speed and cloud cover categories as specified in Table 2 and on the top right of each figure. Wind speed categories are displayed from left to right and cloud cover categories from top to bottom. The annual mean diurnal cycle and uncertainty bars are displayed in black, Southern Hemisphere winter (JJA) in blue, spring (SON) in green, summer (DJF) in red and autumn (MAM) in orange.

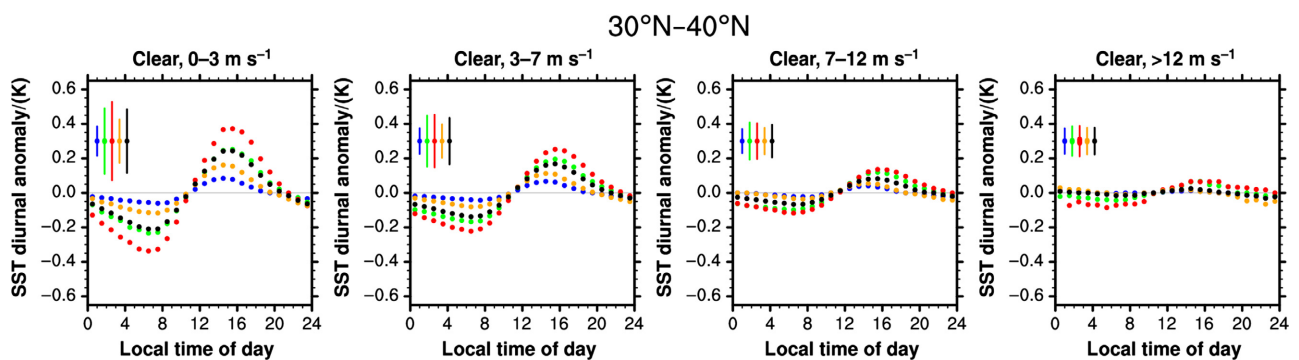


**Figure 4.** Same as top panel of Figure 3 but for the latitudinal band 30°N–40°N. The annual mean diurnal cycle and uncertainty bars are displayed in black, Northern Hemisphere winter (DJF) in blue, spring (MAM) in green, summer (JJA) in red and autumn (SON) in orange.

By construction, the data and fit presented here have zero mean across the day. To estimate the cycle relative to 'foundation SST' (<https://www.ghrsst.org/science->

and-applications/sst-definitions/), find the value of the minimum of the curve in the vicinity of 06 h and subtract this value from the values throughout the day.

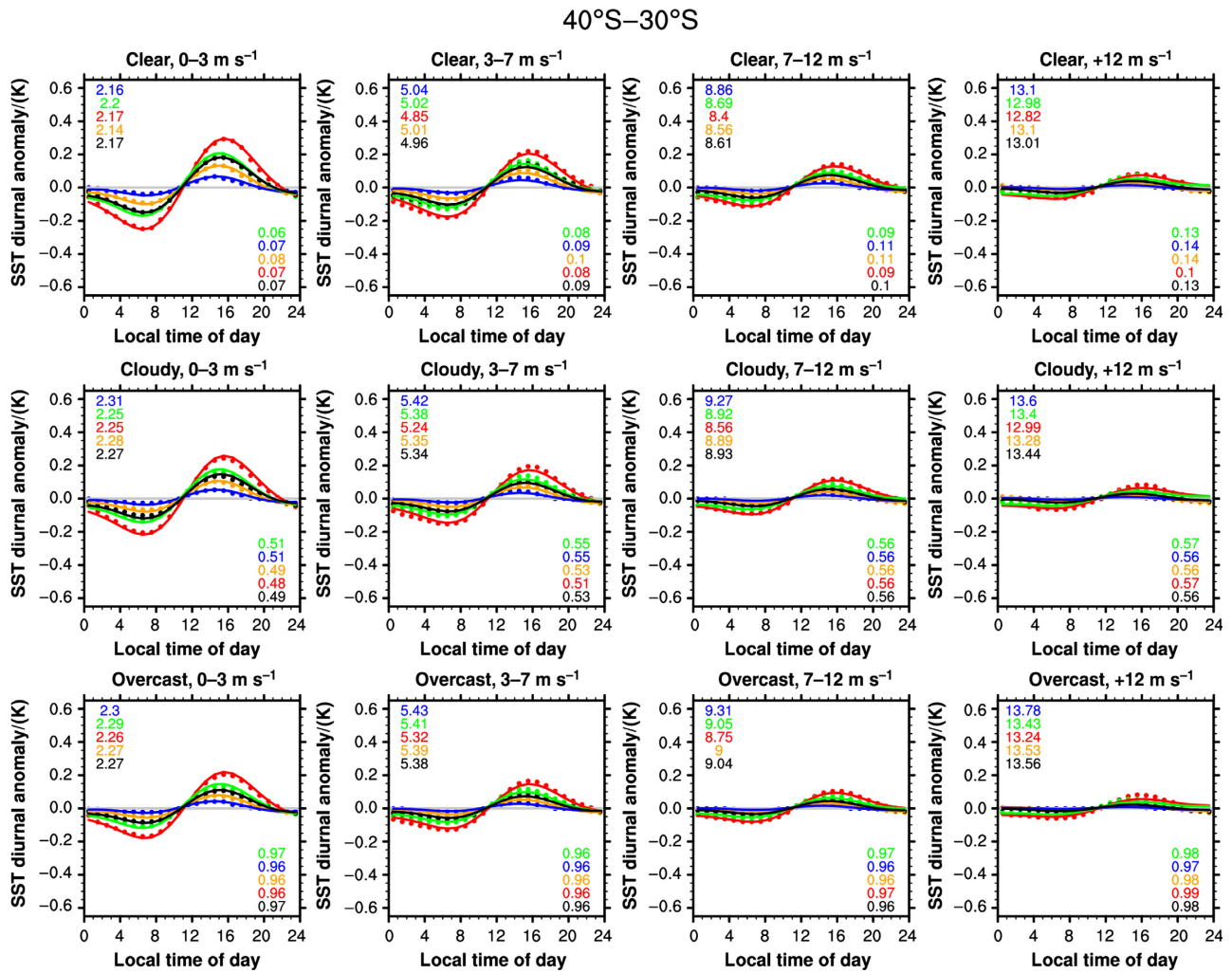


**Figure 5.** Same as Figure 3 but with the fit overlaid as solid line. Values in top left/bottom right corner state the mean wind speed/total cloud cover for the respective category. The annual values are displayed in black, Southern Hemisphere winter (JJA) in blue, spring (SON) in green, summer (DJF) in red and autumn (MAM) in orange.

#### 1.4. Fit evaluation

The fit as shown on the example of the latitudinal bands 40°S–30°S/30°N–40°N in Figures 5 and 6 shows a good agreement with the observed data, with a

standard deviation of the residuals ranging from 0.003K to 0.018K. We estimate the overall fitting uncertainty  $U_{fit}$  by solving the following equation across bin-median-minus-fit residuals of all bins,  $\delta_{bin}$ , for a constant  $U_{fit}$ :

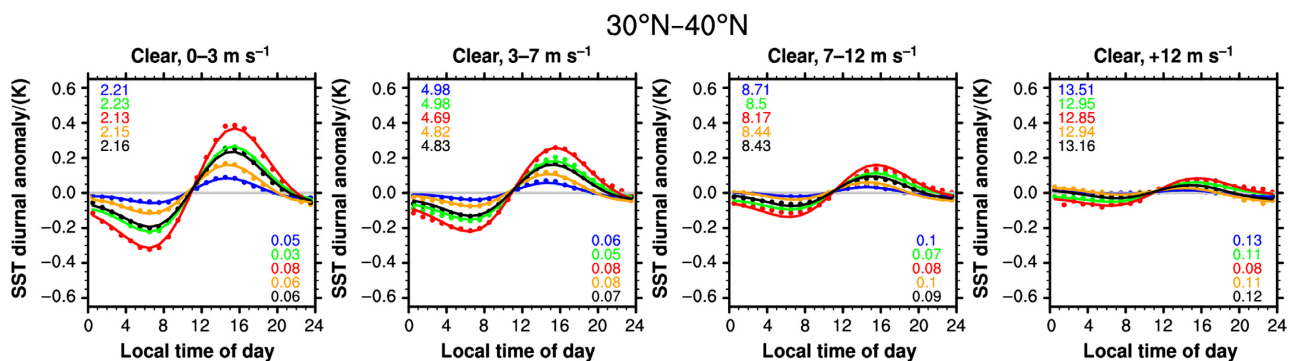


**Figure 6.** Same as top row of Figure 5 but for the latitudinal band 30°N–40°N. The annual mean diurnal cycle is displayed in black, winter (DJF) in blue, spring (MAM) in green, summer (JJA) in red and autumn (SON) in orange.

$$\left( \frac{\delta_{bin}}{\sqrt{U_{bin}^2 + U_{fit}^2}} \right) = 1.$$

The determined fitting uncertainty is 0.0165 K, which is small, but not negligible compared to the statistical uncertainties,  $U_{bin}$ .

By applying fitting all wind and cloud cover bins, simultaneously, we achieve a smooth fit even in case conditions where hourly anomalies are highly uncertain because of relatively few contributing data.

The form of the Equation (1), however, permits some unphysical behaviour: sometimes the fitted curve has a positive (warming) time derivative at the beginning or close of the local day. This effect is not consistent with the observations or typical physical conditions, and is an artefact of the polynomial fitting function. However, in comparison with the amplitude of the diurnal SST anomalies, overall, the unphysical temporal evolution in temperature is small.

## 2. Dataset location and format

The datasets of stratified drifting buoy data and of parameters for the diurnal cycle fits are provided in NetCDF format in a single file. This file provides the observed average diurnal SST anomalies, the fitted diurnal SST anomalies, the colocated values of the wind and cloud cover fields used for computing the fitting coefficients as well as the two measures of statistical uncertainty in the observed diurnal SST anomalies.

These empirical fields have four dimensions: latitude band, wind-speed-and-cloud-cover category (Table 2), season and local hour of day.

The fitting parameter field has three dimensions: latitude band, season and the index of the coefficients corresponding to Equation (1). The file metadata are shown below.

```
file global attributes:
Conventions : CF-1.6
title : diurnal SST anomalies from ICOADS v2.5
institute : University of Reading, Reading, UK
author : S Morak-Bozzo
source : ICOADS v2.5 drifting buoy data and ERA
Interim 10m wind speed and total cloud cover
history : Sun 31 Jan 2016 10:38:48 GMT: ncl < all-
none_fit_matrixmultiplication_approach2_20160126.ncl
dimensions:
latitude = 18 // unlimited
category= 12
season = 5
tod = 24
coefficients = 14
variables:
float sstano_obs (latitude, category, season, tod)
units : K
```

```
short_name : observed diurnal SST anomalies
long_name : diurnal SST anomalies from
ICOADS drifter observations 1986–2012
_FillValue : -999
integer latitude (latitude)
long_name : centre of latitude band in degree N
short_name : centre of latitude band in degree N
units : degrees_north
integer category (category)
long_name : clear, 0–3 m/s, clear, 3–7 m/s, clear,
7–12 m/s, clear, >12 m/s, cloudy, 0–3 m/s, cloudy,
3–7 m/s, cloudy, 7–12 m/s, cloudy, >12 m/s, overcast,
0–3 m/s, overcast, 3–7 m/s, overcast, 7–12 m/s,
overcast, >12 m/s
units : 1
integer season (season)
long_name : DJF, MAM, JJA, SON, annual mean
units : 1
float tod (tod)
units : hours
long_name : local time of day, centred on half hour
float sstano_fit (latitude, category, season, tod)
short_name : fitted diurnal SST anomalies
long_name : fitted diurnal SST anomalies following:
y(t)=a(0)+a(1)*u+a(2)*C+a(3)*t+a(4)*t*u+a(5)*t*
C+a(6)*sin(omega*t)*exp(-u/avg(u))
+a(7)*C*sin(omega*t)*exp(-u/avg(u))
+a(8)*cos(omega*t)*exp(-u/avg(u))
+a(9)*C*cos(omega*t)*exp(-u/avg(u))
+a(10)*sin(2*omega*t)*exp(-u/avg(u))
+a(11)*C*sin(2*omega*t)*exp(-u/avg(u))
+a(12)*cos(2*omega*t)*exp(-u/avg(u))
+a(13)*C*cos(2*omega*t)*exp(-u/avg(u))
units : K
_FillValue : -999
float u (latitude, category, season, tod)
units : m/s
long_name : median wind speed per bin
seasons : 5
latbands : 85
_FillValue : -999
float C (latitude, category, season, tod)
units : 1/10
long_name : median total cloud cover per bin
seasons : 5
latbands : 85
_FillValue : -999
float fit_coeffs (latitude, season, coefficients)
short_name : fitting coefficients
long_name : fitting coefficients a_0-a_13
units : 1
_FillValue : -999
integer coefficients (coefficients)
long_name : coefficients a_0-a_13 for equation see
long_name variable sstano_fit
units : 1
float sstano_obs_stdv (latitude, category, season,
tod)
units : K
```

short\_name : robust standard deviation of observed diurnal SST anomalies

long\_name : robust standard deviation of diurnal SST anomalies from ICOADS drifter observations 1986–2012 for each hourly bin

seasons : 5

latbands : 85

\_FillValue : 9.96921e+36

float sstano\_obs\_stderr (latitude, category, season, tod)

units : K

short\_name : robust standard error of observed diurnal SST anomalies

long\_name : robust standard error of diurnal SST anomalies from ICOADS drifter observations 1986–2012 for each hourly bin

seasons : 5

latbands : 85

\_FillValue : 9.96921e+36

The data are available for download from Figshare (<http://dx.doi.org/10.6084/m9.figshare.2069049>).

### 3. Dataset use and reuse

This dataset will help comparing SST values taken at different local times or to estimate the diurnal variability for climatological purposes. It will also serve to constrain or test models of diurnal cycle computation and air-sea interaction at high temporal resolution. It is distributed under a Creative Commons by attribution license, and any published use should refer to this paper.

### Acknowledgements

The research presented in this paper was funded by NERC NE/J02306X/2 and NE/J020788/1. The authors are grateful to reviewers of this manuscript for their helpful comments.

### References

- Clayson CA, Curry JA. 1996. Determination of surface turbulent fluxes for the tropical ocean-atmosphere coupled ocean-atmosphere response experiment: comparison of satellite retrievals and *in situ* measurements. *Journal of Geophysical Research* **101**: 28515–28528.
- Dee DP, Uppala SM, Simmons AJ, Berrisford P, Poli P, Kobayashi S, Andrae U, Balmaseda MA, Balsamo G, Bauer P, Bechtold P, Beljaars ACM, van de Berg L, Bidlot J, Bormann N, Delsol C, Dragani R, Fuentes M, Geer AJ, Haimberger L, Healy SB, Hersbach H, Hólm EV, Isaksen L, Kållberg P, Köhler M, Matricardi M, McNally AP, Monge-Sanz BM, Morcrette J-J, Park B-K, Peubey C, de Rosnay P, Tavolato C, Thépaut J-N, Vitart F. 2011. The ERA-interim reanalysis: configuration and performance of the data assimilation system. *Quarterly Journal of the Royal Meteorological Society* **137**: 553–597, doi:10.1002/qj.828.
- Filipiak MJ, Merchant CJ, Kettle H, Le Borgne P. 2012. A statistical model for sea surface diurnal warming driven by numerical weather predictions fluxes and winds. *Ocean Science*, **8**: 197–209, ISSN 1812-0784, doi:10.5194/os-8-197-2012.
- Gentemann CL, Donlon CJ, Stuart-Menteth A, Wentz FJ. 2003. Diurnal signals in satellite sea surface temperature measurements. *Geophysical Research Letters* **30**: 1140, doi:10.1029/2002GL016291.
- Kawai Y, Kawamura H. 2003. Validation of daily amplitude of sea surface temperature evaluated with a parametric model using satellite data. *Journal of Oceanography* **59**: 637–644.
- Kawai Y, Wada A. 2007. Diurnal sea surface temperature variation and its impact on the atmosphere and ocean. *A Review, Journal of Oceanography* **63**: 721–744.
- Kennedy JJ, Brohan P, Tett SFB. 2007. A global climatology of the diurnal variations in sea-surface temperature and implications for MSU temperature trends. *Geophysical Research Letters* **34**: L05712, doi:10.1029/2006GL028920.
- Lean K, Saunders RW. 2013. Validation of the ATSR reprocessing for climate (ARC) dataset using data from drifting buoys and a three-way error analysis. *Journal of Climate* **26**: 4758–4772.
- Li W, Yu R, Liu H, Yu Y. 2001. Impacts of diurnal cycle of SST on the interseasonal variation of surface heat flux over the western Pacific warm pool. *Advances in Atmospheric Sciences* **18**: 793–806.
- Lindfors AV, Mackenzie IA, Tett SFB, Shi L. 2011. Climatological diurnal cycles in clear-sky brightness temperatures from the high-resolution infrared radiation sounder (HIRS). *Journal of Atmospheric and Oceanic Technology* **28**: 1199–1205, doi:10.1175/JTECH-D-11-00093.1.
- Merchant CJ, Filipiak MJ, Le Borgne P, Roquet H, Autret E, Piolle J-F, Lavender S. 2008. Diurnal warm-layer events in the western Mediterranean and European shelf seas. *Geophysical Research Letters*, **35**: L04601, ISSN 0094-8276, doi:10.1029/2007GL033071.
- Merchant CJ, Embury O, Rayner NA, Berry DI, Corlett G, Lean K, Veal KL, Kent EC, Llewellyn-Jones D, Remedios JJ, Saunders R. 2012. A twenty-year independent record of sea surface temperature for climate from along-track scanning radiometers. *Journal of Geophysical Research*, **117**. C12013, ISSN 0148-0227 doi:10.1029/2012JC008400.
- Morak-Bozzo S. 2015. Diurnal SST anomalies. V1.1. Figshare. doi: 10.6084/m9.figshare.2069049
- Rousseeuw PJ, Croux C. 1993. Alternatives to the median absolute deviation. *Journal of the American Statistical Association* **88**: 1273–1283, doi:10.1080/01621459.1993.10476408.
- Stuart-Menteth AC, Robinson IS, Challenor PG. 2003. A global study of diurnal warming using satellite-derived sea surface temperature. *Journal of Geophysical Research* **108**: 3155, doi:10.1029/2002JC001534.
- Webster PJ, Clayson CA, Curry JA. 1996. Clouds, radiation, and the diurnal cycle of sea surface temperature in the tropical western Pacific. *Journal of Climate* **9**: 1712–1730.

Wilkinson C, Woodruff SD, Brohan P, Claesson S, Freeman E, Koek F, Lubker SJ, Marzin C, Wheeler D. 2011. Recovery of logbooks and international marine data: the RECLAIM project. *International Journal of Climatology* **31**: 968–979, doi:10.1002/joc.2102.

Woodruff SD, Worley SJ, Lubker SJ, Ji Z, Eric Freeman J, Berry DI, Brohan P, Kent EC, Reynolds RW, Smith SR, Wilkinson C. 2011. ICOADS Release 2.5: extensions and enhancements to the surface marine meteorological archive. *International Journal of Climatology* **31**: 951–967, doi:10.1002/joc.2103.